

## Broadband high-efficiency surface-plasmon-polariton coupler with silicon-metal interface

Jie Tian, Shuqing Yu, Wei Yan, and Min Qiu

Citation: *Appl. Phys. Lett.* **95**, 013504 (2009); doi: 10.1063/1.3168653

View online: <http://dx.doi.org/10.1063/1.3168653>

View Table of Contents: <http://apl.aip.org/resource/1/APPLAB/v95/i1>

Published by the [American Institute of Physics](http://www.aip.org).

---

### Related Articles

Repetitive sub-gigawatt rf source based on gyromagnetic nonlinear transmission line  
*Rev. Sci. Instrum.* **83**, 074705 (2012)

Coupling into tapered metal parallel plate waveguides using a focused terahertz beam  
*Appl. Phys. Lett.* **101**, 041109 (2012)

Etch induced microwave losses in titanium nitride superconducting resonators  
*Appl. Phys. Lett.* **100**, 262605 (2012)

Radio frequency charge sensing in InAs nanowire double quantum dots  
*Appl. Phys. Lett.* **100**, 253508 (2012)

Non-contact characterization of graphene surface impedance at micro and millimeter waves  
*J. Appl. Phys.* **111**, 114908 (2012)

---

### Additional information on *Appl. Phys. Lett.*

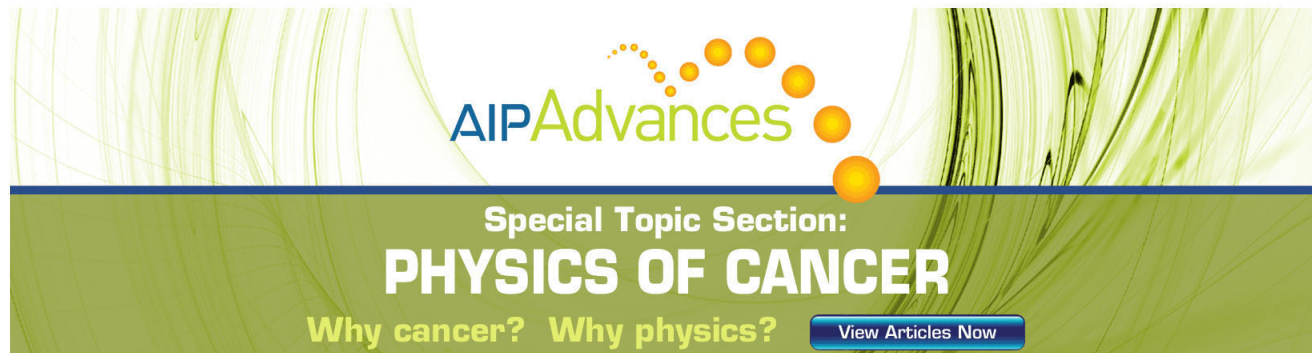
Journal Homepage: <http://apl.aip.org/>

Journal Information: [http://apl.aip.org/about/about\\_the\\_journal](http://apl.aip.org/about/about_the_journal)

Top downloads: [http://apl.aip.org/features/most\\_downloaded](http://apl.aip.org/features/most_downloaded)

Information for Authors: <http://apl.aip.org/authors>

## ADVERTISEMENT

The advertisement features a green and yellow abstract background with flowing lines. At the top, the 'AIP Advances' logo is shown, with 'AIP' in blue and 'Advances' in green, accompanied by a series of orange dots. Below this, the text 'Special Topic Section:' is in white, followed by 'PHYSICS OF CANCER' in large, bold, white capital letters. At the bottom, the phrase 'Why cancer? Why physics?' is written in yellow, and a blue button with the text 'View Articles Now' is positioned to the right.

AIP Advances

Special Topic Section:  
**PHYSICS OF CANCER**

Why cancer? Why physics? [View Articles Now](#)

# Broadband high-efficiency surface-plasmon-polariton coupler with silicon-metal interface

Jie Tian, Shuqing Yu, Wei Yan, and Min Qiu<sup>a)</sup>

Photonics and Microwave Engineering, School of Information and Communication Technology,  
Royal Institute of Technology, Electrum 229, 16440 Kista, Sweden

(Received 5 May 2009; accepted 11 June 2009; published online 7 July 2009)

A high efficiency surface plasmonic coupler composed of a tapered silicon strip waveguide and a subwavelength scale metal gap waveguide is experimentally demonstrated. By tuning the parameters of the taper and the metal gap, the theoretical coupling efficiencies can be as high as 88% for a wide wavelength range. A silicon-gold plasmonic coupler is then fabricated, demonstrating **35% coupling efficiency** per facet. Our experimental demonstration is a crucial step for hybrid integration of plasmonic components with conventional dielectric components. © 2009 American Institute of Physics. [DOI: [10.1063/1.3168653](https://doi.org/10.1063/1.3168653)]

Plasmonic devices, which allow subwavelength confinement for optical mode, have shown the tremendous potential applications in ultracompact photonic integrated circuits.<sup>1–5</sup> Several different plasmonic circuit components, which could be much smaller than the light wavelength, have been proposed or demonstrated, such as metallic nanowires,<sup>6</sup> channel waveguides,<sup>7–9</sup> resonators,<sup>10</sup> beam splitters,<sup>11,12</sup> Mach–Zehnder interferometers,<sup>13</sup> sharp bends,<sup>12</sup> etc. However, one fundamental issue still not completely solved is how to efficiently couple light from conventional optical waveguides (e.g., fibers or silicon wire waveguides) into plasmonic waveguides. There are two general schemes which are used to couple light into plasmonic structures.<sup>14</sup> The most widely used one is through momentum matching. The external light usually has largely different momentum than those of plasmonic waves. An efficient free-space coupling method must provide the momentum difference. The matching can be obtained by a number of methods, such as prism coupling,<sup>15,16</sup> grating coupling,<sup>17</sup> and nanoparticle scattering.<sup>18</sup> Those methods always require large scale (larger than the wavelength) devices, such as the grating coupler with more than 10  $\mu\text{m}$  dimensions, and the transmission bandwidth is usually limited. The other scheme for coupling is through field matching across the interface, i.e., end-fire coupling.<sup>19,20</sup> The method could be highly efficient and broadband. Recently, a modulated-index metal-slot waveguide transfer with lateral mode confinement and a squeezing light coupler with vertical mode confinement have been investigated theoretically.<sup>21–23</sup> The calculated coupling efficiency can be as high as 95%. However, only a few experimental demonstrations of light coupling from a dielectric waveguide into plasmonic tapers have been shown,<sup>24</sup> mostly due to the fact that the footprint of a plasmonic waveguide is much smaller than that of a dielectric waveguide, thus efficient coupling is difficult to achieve.

In the present letter, we experimentally demonstrate a planar plasmonic coupler coupling light between a silicon wire waveguide and a metal-dielectric-metal plasmonic gap waveguide. The theoretical maximum coupling efficiency is 88% for the gold waveguide. The experiment results give a broadband coupling efficiency as high as 35%.

The schematic picture of the plasmonic coupler structure is shown in Fig. 1(a). The whole structure is based on the silicon-on-insulator (SOI) platform. The coupler is composed of two tapered silicon strip waveguides and a plasmonic gap waveguide, which extends symmetrical bevel edge that are parallel with the silicon taper edges. The strip silicon waveguide has a 450-nm-wide by a 250-nm-high rectangular cross section, which are typical parameters for single mode silicon wire waveguides. The thickness of the metal material slabs for forming the plasmonic gap waveguide is 250 nm, the same as that of the silicon tapered waveguide. Figure 1(b) indicates the taper coupler parameters from the top view. The light mode coupling between the silicon taper and the gold film and the light propagation in the plasmonic gap are shown in Fig. 1(c). Figure 1(d) is the optical microscope image of the structure. A scanning electron micrograph (SEM) of a gold plasmonic coupler is shown in Fig. 1(e).

For the design and optimization of the silicon-metal tapered coupler, the three-dimensional finite-difference time-domain (3D FDTD) method is used to simulate the coupling efficiency per facet as the function of the wavelength. Only the transverse electric-polarized mode (the electric field is parallel to sample surface plane) is excited here. The crucial part of the coupler is the taper, thus three essential parameters were considered: the angle  $\theta$ , the taper width  $d$ , and the distance  $l$  [see Fig. 1(b)]. We choose the gold material as the plasmonic waveguide. The dielectric strip waveguide with a taper is made of silicon. The whole structure is placed on silica substrate, and the background medium material is air. First, we fix the plasmonic waveguide as  $w=100$  nm,  $\theta=10^\circ$ , and  $l=0$   $\mu\text{m}$ . Four different taper widths  $d$  (20, 40, 60, and 80 nm) are investigated. From Fig. 2(a), we can see that the coupling efficiencies increase as the taper width decrease, the maximum coupling efficiency is about 84% from the sharper taper,  $d=20$  nm. Second, the plasmonic waveguide is fixed as  $w=200$  nm,  $\theta=10^\circ$ , and  $l=0.25$   $\mu\text{m}$ . The taper width  $d$  varies from 80 to 200 nm. From Fig. 2(b), we can see that the coupling efficiencies increase as the taper width increase. For instance, the maximum coupling efficiency is 88% from the wider taper  $d=200$  nm. The inset graphs in Fig. 2 show that all the coupling light have been confined in the plasmonic waveguide. For the comparison, the coupling efficiency for the same coupler structure with

<sup>a)</sup>Electronic mail: min@kth.se.

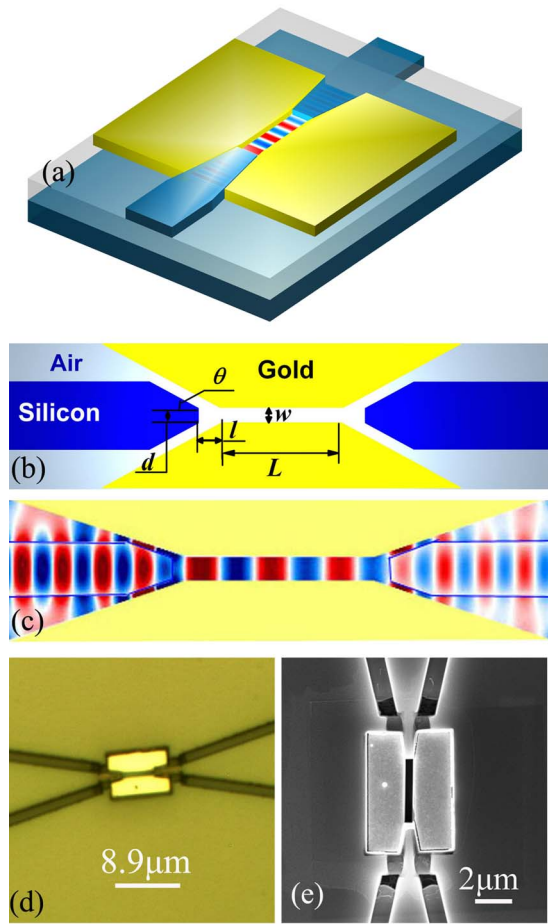


FIG. 1. (Color online) Two tapered silicon strip waveguides coupled with a plasmonic gap waveguide. (a) The schematic picture of the silicon-metal plasmonic coupler. (b) The top-view with the taper parameters:  $\theta$  is the angle between the taper and the center axis of silicon waveguide (the plasmonic taper edge is set to be parallel to the silicon taper),  $d$  is the width of the silicon taper end, and  $l$  is the distance between the end of silicon waveguide and the start of the plasmonic waveguide.  $w$  and  $L$  are the width and length of the waveguide gap, respectively. (c) The hertz field distribution at the wavelength  $1.5 \mu\text{m}$  simulated by 3D FDTD. (d) Optical microscope image of a fabricated silicon-gold plasmonic coupler ( $\theta=10^\circ$ ,  $d=200 \text{ nm}$ ,  $l=0.25 \mu\text{m}$ ,  $w=200 \text{ nm}$ , and  $L=3 \mu\text{m}$ ). (e) The SEM of the fabricated taper.

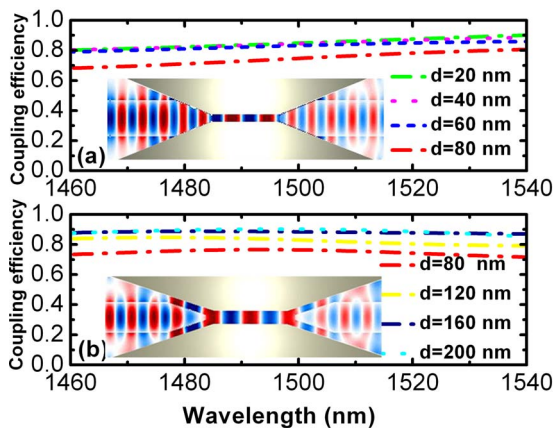


FIG. 2. (Color online) 3D FDTD results of coupler structures with gold waveguide. (a)  $w=100 \text{ nm}$ ,  $\theta=10^\circ$ ,  $l=0 \mu\text{m}$ ,  $d$  various from 20 to 80 nm. (b)  $w=200 \text{ nm}$ ,  $\theta=10^\circ$ ,  $l=0.25 \mu\text{m}$ ,  $d$  various from 80 to 200 nm. (The inset is the mode distribution in the coupler).

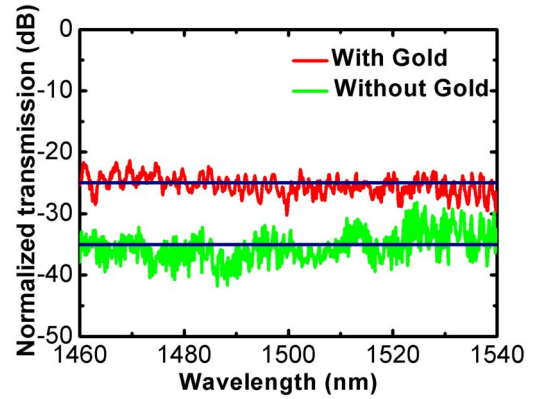


FIG. 3. (Color online) The normalized transmission spectrum before and after the formation of the gold plasmonic gap waveguide.

the closed gap (i.e., the gap filled with metal) is calculated, which is lower than 1.1%. From Fig. 2, it is also worth noting that the coupling efficiency is extremely broadband, almost independent of wavelengths.

In the experiment, the fabricated sample parameters are  $w=200 \text{ nm}$ ,  $\theta=10^\circ$ ,  $l=0.25 \mu\text{m}$ , and  $d=200 \text{ nm}$  with different plasmonic lengths  $L$ . We fabricate the coupler in a five-step process. First, the silicon strip waveguides with the taper were directly written on a SOI wafer with a 250 nm silicon top layer and 3  $\mu\text{m}$  Buried Oxide layer by a Quanta 3D FEG dual-beam field-emission-gun (FIB) system, where an additional 50 nm thick aluminum oxide ( $\text{Al}_2\text{O}_3$ ) on the top silicon acting as an etching mask. Next, a rapid thermal annealing (RTA) treatment was performed to remove the implanting gallium ions and to recrystallize the amorphous layer induced by FIB. RTA was conducted at  $1000^\circ$  for 30 s in  $\text{N}_2$  atmosphere. Third, the device window for metal evaporation was opened by FIB on a bilayer photoresist structure. Note that, a merit of the FIB is that it has sufficient precision alignment in the window opening step. For the metal waveguide, we opt for gold because it does not oxidize and has good plasmon response in the near-infrared part of the electromagnetic spectrum, that is, the high coupling efficiency can be obtained while the propagation losses are moderate. Fourth, a prior layer of 3 nm thick titanium for adhesion between the gold and the silica, and then a 250 nm thick gold film were deposited by electron-beam evaporation. Finally, lift-off was performed in acetone to obtain the final structure. The SEM picture of the fabricated metal-silicon-metal tapered coupler structure is shown in Fig. 1(e).

Figure 3 shows the normalized transmission before and after the formation of the gold plasmonic gap waveguide. The gold waveguide is  $L=5 \mu\text{m}$  long. The transmission spectrum is normalized by a reference single mode silicon waveguide with  $450 \times 250 \text{ nm}$  core size. From Fig. 3, we can see that the average transmission power before and after the gold formation is  $-35$  and  $-25 \text{ dB}$ , respectively. The enhancement power is proximate 10 dB by comparing two reference lines.

To determine the coupling efficiency and the propagation loss, gold waveguides with different length  $L$  but with the same tapered coupler structure were fabricated and measured. Figure 4(a) plots the measured transmission for various waveguide lengths. From the plot, we can estimate the values of the propagation loss and coupling efficiency, and they are  $2.9 \text{ dB}/\mu\text{m}$  and  $5.5 \text{ dB}$  (28%)/facet at wavelength



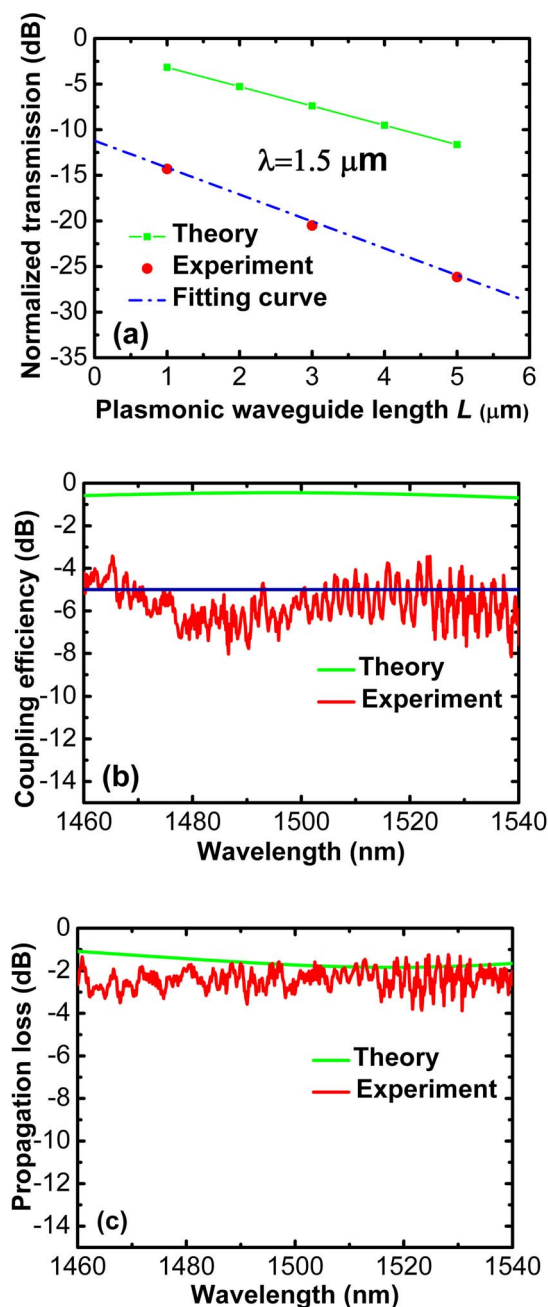


FIG. 4. (Color online) The theoretical and experiment results of the coupling efficiency and the propagation loss. (a) Normalized transmission vs the length of the slot waveguide at wavelength  $1.5 \mu\text{m}$ . (b) Coupling efficiency per facet as the function of the wavelength. (c) Propagation loss in the slot waveguide as the function the wavelength.

around  $1.5 \mu\text{m}$ , respectively. Figure 4(b) shows the measured coupling efficiency per facet as the function of the wavelength. From Fig. 4(b), we can see the average coupling efficiency is about 4.5 dB (35%). The simulation result of the structure is added for comparison. The discrepancy between

the simulation and experimental results in terms of efficiency is caused by the gold pattern defects and roughness and also due to the fact that the gold waveguide is not perfectly aligned to the silicon taper. In Fig. 4(c) we show the propagation loss in the gap waveguide versus the wavelength. The average loss is about  $-2.5 \text{ dB}/\mu\text{m}$ , compared with the simulation results  $-1.5 \text{ dB}/\mu\text{m}$ , demonstrating a relatively good agreement between the two.

In conclusion, we have studied a plasmonic coupler with high efficiency coupling between the silicon waveguide and the plasmonic waveguide. By tuning the silicon taper and the plasmonic waveguide parameters, we can simultaneously achieve subwavelength confinement and high (theoretically 88%) coupling efficiency. We have further shown the experimental demonstration of 35% coupling efficiency in a silicon-gold coupled structure. This silicon-metal coupling structure enables the potential application in the hybrid integration of semiconductor devices and plasmonics.

This work is supported by the Swedish Foundation for Strategic Research (SSF) and the Swedish Research Council (VR).

- <sup>1</sup>W. L. Barnes, A. Dereux, and T. W. Ebbesen, *Nature (London)* **424**, 824 (2003).
- <sup>2</sup>E. Ozbay, *Science* **311**, 189 (2006).
- <sup>3</sup>B. Min, E. Ostby, V. Sorger, E. U. Avila, L. Yang, X. Zhang, and K. Vahala, *Nature (London)* **457**, 455 (2009).
- <sup>4</sup>L. Verslegers, P. B. Catrysse, Z. Yu, J. S. White, E. S. Barnard, M. L. Brongersma, and S. Fan, *Nano Lett.* **9**, 235 (2009).
- <sup>5</sup>S. A. Maier, P. G. Kik, H. A. Atwater, S. Meltzer, E. Harel, B. E. Koel, and A. A. G. Requicha, *Nature Mater.* **2**, 229 (2003).
- <sup>6</sup>A. W. Sanders, D. A. Routenberg, B. J. Wiley, Y. Xia, E. R. Dufresne, and M. A. Reed, *Nano Lett.* **6**, 1822 (2006).
- <sup>7</sup>E. Verhagen, J. A. Dionne, L. Kuipers, H. A. Atwater, and A. Polman, *Nano Lett.* **8**, 2925 (2008).
- <sup>8</sup>T. Holmgaard, S. I. Bozhevolnyi, L. Markey, A. Dereux, A. V. Krasavin, P. Bolger, and A. V. Zayats, *Phys. Rev. B* **78**, 165431 (2008).
- <sup>9</sup>A. J. Dionne, H. J. Lezec, and H. A. Atwater, *Nano Lett.* **6**, 1928 (2006).
- <sup>10</sup>S. Xiao and N. A. Mortensen, *Opt. Express* **16**, 14997 (2008).
- <sup>11</sup>T. Holmgaard, Z. Chen, S. I. Bozhevolnyi, L. Markey, A. Dereux, A. V. Krasavin, and A. V. Zayats, *Opt. Express* **16**, 13585 (2008).
- <sup>12</sup>G. Veronis and S. Fan, *Appl. Phys. Lett.* **87**, 131102 (2005).
- <sup>13</sup>S. I. Bozhevolnyi, V. S. Volkov, E. Devaux, J. Y. Laluet, and T. W. Ebbesen, *Nature (London)* **440**, 508 (2006).
- <sup>14</sup>T. W. Ebbesen, C. Genet, and S. I. Bozhevolnyi, *Phys. Today* **61**, 44 (2008).
- <sup>15</sup>W. D. Wilson, *Science* **295**, 2103 (2002).
- <sup>16</sup>W. P. Chen and J. M. Chen, *J. Opt. Soc. Am.* **71**, 189 (1981).
- <sup>17</sup>S. Scheerlinck, J. Schrauwen, F. V. Laere, D. Taillaert, D. V. Thourhout, and R. Baets, *Opt. Express* **15**, 9625 (2007).
- <sup>18</sup>L. Eurenium, C. Hägglund, E. Olsson, B. Kasemo, and D. Chakarov, *Nat. Photonics* **2**, 360 (2008).
- <sup>19</sup>G. Veronis and S. Fan, *Opt. Express* **15**, 1211 (2007).
- <sup>20</sup>G. I. Stegeman, R. F. Wallis, and A. A. Maradudin, *Opt. Lett.* **8**, 386 (1983).
- <sup>21</sup>N. N. Feng and L. D. Negro, *Opt. Lett.* **32**, 3086 (2007).
- <sup>22</sup>P. Ginzburg, D. Arbel, and M. Orenstein, *Opt. Lett.* **31**, 3288 (2006).
- <sup>23</sup>R. Yang, M. A. G. Abushagur, and Z. Lu, *Opt. Express* **16**, 20142 (2008).
- <sup>24</sup>L. Chen, J. Shakya, and M. Lipson, *Opt. Lett.* **31**, 2133 (2006).